

Published in final edited form as:

Cell Physiol Biochem. 2016 ; 39(4): 1404–1420. doi:10.1159/000447844.

## Resveratrol Specifically Kills Cancer Cells by a Devastating Increase in the Ca<sup>2+</sup> Coupling Between the Greatly Tethered Endoplasmic Reticulum and Mitochondria

Corina T. Madreiter-Sokolowski<sup>a</sup>, Benjamin Gottschalk<sup>a</sup>, Warisara Parichatikanond<sup>a,b</sup>, Emrah Eroglu<sup>a</sup>, Christiane Klec<sup>a</sup>, Markus Waldeck-Weiermair<sup>a</sup>, Roland Malli<sup>a</sup>, and Wolfgang F. Graier<sup>a</sup>

<sup>a</sup>Institute of Molecular Biology and Biochemistry, Medical University of Graz, Graz, Austria

<sup>b</sup>Department of Pharmacology, Faculty of Pharmacy, Mahidol University, Bangkok, Thailand

### Abstract

**Background/Aims**—Resveratrol and its derivative piceatannol are known to induce cancer cell-specific cell death. While multiple mechanisms of actions have been described including the inhibition of ATP synthase, changes in mitochondrial membrane potential and ROS levels, the exact mechanisms of cancer specificity of these polyphenols remain unclear. This paper is designed to reveal the molecular basis of the cancer-specific initiation of cell death by resveratrol and piceatannol.

**Methods**—The two cancer cell lines EA.hy926 and HeLa, and somatic short-term cultured HUVEC were used. Cell viability and caspase 3/7 activity were tested. Mitochondrial, cytosolic and endoplasmic reticulum Ca<sup>2+</sup> as well as cytosolic and mitochondrial ATP levels were measured using single cell fluorescence microscopy and respective genetically-encoded sensors. Mitochondria-ER junctions were analyzed applying super-resolution SIM and ImageJ-based image analysis.

**Results**—Resveratrol and piceatannol selectively trigger death in cancer but not somatic cells. Hence, these polyphenols strongly enhanced mitochondrial Ca<sup>2+</sup> uptake in cancer exclusively. Resveratrol and piceatannol predominantly affect mitochondrial but not cytosolic ATP content that yields in a reduced SERCA activity. Decreased SERCA activity and the strongly enriched tethering of the ER and mitochondria in cancer cells result in an enhanced MCU/Letm1-dependent mitochondrial Ca<sup>2+</sup> uptake upon intracellular Ca<sup>2+</sup> release exclusively in cancer cells. Accordingly, resveratrol/piceatannol-induced cancer cell death could be prevented by siRNA-mediated knock-down of MCU and Letm1.

---

This article is licensed under the Creative Commons Attribution-NonCommercial-NoDerivatives 4.0 International License (CC BY-NC-ND) (<http://www.karger.com/Services/OpenAccessLicense>). Usage and distribution for commercial purposes as well as any distribution of modified material requires written permission.

Wolfgang F. Graier, Ph.D., Institute of Molecular Biology and Biochemistry, Medical University of Graz, Harrachgasse 21/3, 8010 Graz, (Austria), wolfgang.graier@medunigraz.at.

#### Disclosure Statement

The authors declare no conflict of interest.

**Conclusions**—Because their greatly enriched ER-mitochondria tethering, cancer cells are highly susceptible for resveratrol/piceatannol-induced reduction of SERCA activity to yield mitochondrial  $\text{Ca}^{2+}$  overload and subsequent cancer cell death.

## Keywords

Mitochondria; Endoplasmic reticulum; Calcium signaling; Mitochondria-ER coupling; SERCA

## Introduction

Resveratrol is a natural phenol in several plants like grapes [1–3] and mulberries [4, 5]. This compound is known as antioxidant and to exhibit counteracting efficiency against cancer [6], inflammation [7], and aging [8]. Remarkably, resveratrol and its derivative piceatannol [9] specifically cause cell death in cancer cells [10–14]. Different mechanisms including inhibition of respiratory chain complexes [15] and the F1 subunit of ATP synthase [16, 17], changes in ROS levels [18–21], dissipation of mitochondrial membrane potential [13], and  $\text{Ca}^{2+}$  release from the endoplasmic reticulum (ER) [22] have been discussed as possible mechanisms for cancer cell death that is triggered by increased caspase activity, cytochrome c release and, finally, apoptosis [23].

One hallmark of cancer cells is the very high ATP demand of the ER due to the enormous protein folding activity in this organelle [24, 25]. Notably, a cancer-specific functional arrangement between the ER and mitochondria as ATP supplier has been discussed and an improved inter-organelle shuttling of  $\text{Ca}^{2+}$  from the ER into the mitochondria where it enhances the production of ATP is proposed [26]. Subsequently, increased mitochondrial ATP may be shuttled into the ER [27], where it meets the excessive ATP demand of the ER in a cancer cell [24, 25]. The transfer of the ubiquitous second messenger  $\text{Ca}^{2+}$  into the mitochondrial matrix is an important signaling process that substantially contributes to physiological and pathophysiological pathways. For instance, metabolic activity is strongly influenced by  $\text{Ca}^{2+}$ -dependent enzymes of the tricarboxylic acid (TCA) cycle like pyruvate dehydrogenase, isocitrate dehydrogenase, and alpha-ketoglutarate dehydrogenase [28]. Furthermore, mitochondrial  $\text{Ca}^{2+}$  import causes changes in mitochondrial membrane potential [29]. Mitochondria also buffer local  $\text{Ca}^{2+}$  signals and, therefore, regulate  $\text{Ca}^{2+}$  concentration in cellular microdomains [30]. However, mitochondrial  $\text{Ca}^{2+}$  accumulation can have a harmful effect, as it may lead to the opening of the mitochondrial permeability transition pore (PTP), which causes the release of cytochrome c facilitating the formation of the apoptosome and the activation of caspases [31]. Thus, in view of the potential risk of mitochondrial  $\text{Ca}^{2+}$  overload leading to apoptosis and the signaling function of mitochondrial  $\text{Ca}^{2+}$  uptake to stimulate the organelle, mitochondrial  $\text{Ca}^{2+}$  uptake needs to be precisely regulated.

The predominant part of  $\text{Ca}^{2+}$  sequestered by mitochondria is released by inositol 1,4,5-trisphosphate ( $\text{IP}_3$ ) from the internal  $\text{Ca}^{2+}$  store, the ER [32, 33]. ER  $\text{Ca}^{2+}$  release generates  $\text{Ca}^{2+}$  hot spots that approach the mitochondrial surface [34]. This  $\text{Ca}^{2+}$  interplay between mitochondria and ER occurs mostly in specialized regions of the ER called mitochondria-associated ER membranes (MAMs) [35], where ER tubules are closely tethered to

mitochondria by linking proteins like Mfn 2 [36, 37], Grp75 [38], and PACS2 [39]. Within this highly specialized region, a sophisticated toolkit consisting of the IP<sub>3</sub> receptor, the sarco/endoplasmic reticulum Ca<sup>2+</sup> ATPase (SERCA), the mitochondrial Ca<sup>2+</sup> uniplex [40, 41], and the mitochondrial Na<sup>+</sup>/Ca<sup>2+</sup> exchanger (NCLX) [42] controls ER Ca<sup>2+</sup> release and re-uptake as well as mitochondrial Ca<sup>2+</sup> sequestration and extrusion, respectively. The mitochondrial Ca<sup>2+</sup> uniplex consists of the pore forming proteins MCU [43, 44], MCUb [45], EMRE [46], MCUR1 [47, 48], MICU1 [49], and MICU2 [50]. Importantly, the activity of the mitochondrial Ca<sup>2+</sup> uniplex is under the control of intermembrane Ca<sup>2+</sup> that binds to the gatekeeping MICU1 [51] leading to its rearrangement [52] with a K<sub>D</sub> of 4.4 μM free Ca<sup>2+</sup> and, subsequently, the influx of Ca<sup>2+</sup> into the mitochondrial matrix [53]. Accordingly, the activity of mitochondrial Ca<sup>2+</sup> uptake from the MAM region correlates with the local Ca<sup>2+</sup> concentration that is under the control of SERCA [54].

Considering the reported effects of resveratrol and piceatannol on the F1 subunit of ATP synthase, we hypothesize that these polyphenols trigger cancer cell death by turning the cancer cell-specific MAM arrangement into a suicide machinery. According to our hypothesis, the reduced ATP formation may decrease SERCA activity within MAMs leading eventually to excessive mitochondrial Ca<sup>2+</sup> uptake triggering mitochondrial Ca<sup>2+</sup> overload and, thus, the initiation of the apoptotic pathway in the cancer cell. The current study was designed to challenge this hypothesis by comparing the effects of resveratrol and piceatannol on cell survival and apoptosis, mitochondrial Ca<sup>2+</sup> homeostasis, and (sub)cellular ATP dynamics of primary somatic cells with cancer cell lines.

## Material and Methods

### Chemicals and buffer solutions

Cell culture materials were obtained from PAA laboratories (Pasching, Austria). Oligomycin A, histamine, 2,5-di-t-butyl-1,4-benzohydroquinone (BHQ), and ethylene glycol tetraacetic acid (EGTA) were purchased from Sigma Aldrich (Vienna, Austria), thapsigargin, piceatannol, and resveratrol from Abcam (London, UK). Prior to experiments, cells were washed and maintained for 20 minutes in a HEPES-buffered solution containing 138 mM NaCl, 5 mM KCl, 2 mM CaCl<sub>2</sub>, 1 mM MgCl<sub>2</sub>, 1 mM HEPES, 2.6 mM NaHCO<sub>3</sub>, 0.44 mM KH<sub>2</sub>PO<sub>4</sub>, 0.34 mM Na<sub>2</sub>HPO<sub>4</sub>, 1 mM D-glucose, 0.1% vitamins, 0.2% essential amino acids, and 1% penicillin-streptomycin, the pH of which was adjusted to 7.4 with NaOH or HCl. During the experiments cells were perfused with a Ca<sup>2+</sup>-containing buffer, which consisted of 145 mM NaCl, 5 mM KCl, 2 mM CaCl<sub>2</sub>, 1 mM MgCl<sub>2</sub>, 10 mM D-glucose and 10 mM HEPES, pH adjusted to 7.4, or with a Ca<sup>2+</sup>-free buffer, in which CaCl<sub>2</sub> was replaced by 1 mM EGTA.

### Cell culture and transfection

HeLa and Ea.hy926 cells were grown in Dulbecco's Modified Eagle Medium (Sigma Aldrich) containing 10% fetal bovine serum, 100 U/ml penicillin, 100 μg/ml streptomycin, and 2 mM glutamine (Gibco/LifeTechnologies, Vienna, Austria). For Ca<sup>2+</sup> imaging, cells were plated on 30-mm glass coverslips and transiently transfected at 60 – 80% confluence with 1.5 μg plasmid DNA encoding the appropriate sensor or AKAP-CAAX-RFP as well as,

if necessary, in combination with 100  $\mu$ M siRNA using 2.5  $\mu$ l of TransFast™ transfection reagent (Promega, Madison, WI, USA) in 1 ml of serum- and antibiotic-free medium. Cells were maintained in a humidified incubator (37°C, 5% CO<sub>2</sub>, 95% air) for 16 – 20 hours. Afterwards, transfection mix was replaced by culture medium with supplements. All experiments were performed 48 hours after transfection. siRNAs were obtained from Microsynth (Balgach, Switzerland), and their sequences (5′-3′) were as follows: human MCU siRNA-1: 5′ GCC AGA GAC AGA CAA UAC U dTdT 3′; human MCU siRNA-2: 5′ GGA AAG GGA GCU UAU UGA A dTdT 3′; human UCP2 siRNA: 5′ GCA CCG UCA AUG CCU ACA A dTdT 3′; human UCP3 siRNA: 5′ GGA ACU UUG CCC AAC AUC A dTdT 3′; human Letm1 siRNA-1: 5′ UCC ACA UUU GAG ACU CAG U dTdT 3′; human Letm1 siRNA-2: 5′ AUG UUC CAU UUG GCU GCU G dTdT 3′.

Human umbilical vein endothelial cells (HUVECs) were cultured in endothelial cell growth medium (EGM-2) (Lonza, Basel, Switzerland). For imaging experiments HUVECs were seeded on Poly-L-Lysin coated 30-mm glass coverslips in 6-well plates and infected with BacMam 4mtD3cpv virus (Gibco/LifeTechnologies) following the CellLight protocol. Experiments were performed 48 hours after transfection. Prior approval was obtained for human cell and tissue sample collection from the Institutional Review Board of the Medical University of Graz (protocols 19-252 ex 07/08, 18-243 ex 06/07, 21.060 ex 09/10). Umbilical cords were collected after written informed consent by the mothers after full-term pregnancies in accordance with the Declaration of Helsinki.

### mRNA Isolation and Real Time PCR

Total RNA was isolated using the PEQLAB total RNA isolation kit (PEQLAB Biotechnologie GmbH, Erlangen, Germany), and reverse transcription was performed in a thermal cycler (PEQLAB Biotechnologie GmbH) using a cDNA synthesis kit (Applied Biosystems, Foster City, CA, USA). Expression of MCU, UCP2, UCP3, Letm1, and AKAP-RFP-CAAX in HeLa cells was examined by RT-PCR. A QuantiFast SYBR Green RT-PCR kit (Qiagen, Hilden, Germany) was used to perform real time PCR on a LightCycler 480 (Roche Diagnostics, Vienna, Austria), and data were analyzed by the REST Software (Qiagen). Relative expression of specific genes was normalized with GAPDH as a housekeeping gene. Primers for real time PCR were obtained from Invitrogen (Vienna, Austria), and their sequences (5′-3′) were:

human	MCU	forward, TCCTGGCAGAATTTGGGAG;
human	MCU	reverse, AGAGATAGGCTTGAGTGTGAAC;
human	UCP2	forward, TCCTGAAAGCCAACCTCATG;
human	UCP2	reverse, GGCAGAGTTCATGTATCTCGTC;
human	UCP3	forward, AGAAAATACAGCGGGACTATGG;
human	UCP3	reverse, CTGAGGATGTCGTAGGTCAC;
human	Letm1	forward, TGTTGCTGTGAAGCTCTTCC;
human	Letm1	reverse, TGTTCCTCAAGGCCATCTCC;
mouse	AKAP1	forward, CTCCTTGGCTGGTCCTCCTI;

mouse AKAP1 reverse, ACTCCTTGATGACGCCTCG.

### FRET measurements using genetically encoded sensors

Dynamic changes in  $[Ca^{2+}]_{mito}$ ,  $[Ca^{2+}]_{ER}$ ,  $[ATP]_{cyt}$ , and  $[ATP]_{mito}$  were followed in cells expressing the 4mtD3cpv, D1ER, cytAT1.03, and mtAT1.03 (NGFI, *ngfi.eu*, Graz, Austria), respectively. Culture medium was removed and cells were kept in a HEPES-buffered solution described above. Single cell measurements were performed on a Zeiss AxioVert inverted microscope (Zeiss, Göttingen, Germany) equipped with a polychromator illumination system (VisiChrome; Visitron Systems, Puchheim, Germany) and a thermoelectric-cooled CCD camera (CoolSNAP HQ; Photometrics, Tucson, AZ, USA). Transfected cells were imaged with a 40× oil-immersion objective (Zeiss). Excitation of the fluorophores was at  $440 \pm 10$  nm (440AF21; Omega Optical, Brattleboro, VT, USA), and emission was recorded at 480 and 535 nm using emission filters (480AF30 and 535AF26; Omega Optical) mounted on a Ludl filterwheel. Devices were controlled and data were acquired by VisiView 2.0.3 (Visitron Systems) software and analyzed with GraphPad Prism version 5.0 for Windows (GraphPad Software, La Jolla, CA, USA). Results of FRET measurements are shown as  $(R_i - \text{Background}) + [(R_i - \text{Background}) - (R_0 - \text{Background})]$  (whereas  $R_0$  is the basal ratio) to correct for photobleaching and/or photochromism.

### 3D-Colocalisation analysis

Ea.hy926 and HUVECs were seeded on 24-mm glass coverslips and transfected with D1ER using TransFast™ transfection reagent or BacMaM D1ER virus (Gibco/LifeTechnologies), respectively, according to manufacturer's instructions. After two days, Ea.hy926 and HUVECs were stained for 10 min with 200 nM MitoTracker® Red CMXRos (Invitrogen) and imaged with 488 nm laser excitation (D1ER) and an 561 nm laser with a CFI SR ApoChromat TIRF 100×oil (NA1.49) objective mounted on a Nikon-Structured Illumination Microscopy (N-SIM; Nikon, Tokyo, Japan) system equipped with an Andor iXon3 EMCCD camera. 3D-SIM was used in both channels with very short 30 ms exposure time per image. SIM images were reconstructed using Nis-Elements (Nikon). Images were background corrected with an ImageJ-Plugin (Mosaic Suite, background subtractor). Further, the ImageJ/Fiji tool coloc2 was used to determine Mander's coefficients whereby images were thresholded with Costes automatic threshold to determine Mander's 2 coefficient (overlap of mitochondria with endoplasmic reticulum).

HeLa cells were seeded on 30-mm round coverslips and transfected after two days with mtDsRed/D1ER (1:1) or mtDsRed/D1ER/mAKAP-RFP-CAAX (1:1:3) using TransFast™ transfection reagent. After two days confocal image stacks were acquired with a Zeiss Observer Z.1 inverted microscope equipped with a Yokogawa CSU-X1 Nipkow spinning disk system, a piezoelectric z-axis motorized stage (CRWG3-200; Nippon Thompson Co., Ltd., Tokyo, Japan), and a CoolSNAP HQ2 CCD Camera (Photometrics). Cells expressing D1ER and mtDsRED were excited with 488 nm and 568 nm laser lines (Visitron Systems) with exposure times of 50 - 300 ms using an alpha Plan-Fluar 100x/1.45 Oil M27 (Zeiss). Stacks of 40 – 70 images with 0.15 μm step width were acquired. Stacks were automatically

background corrected and blind-deconvolved using Huygens 2.4.1 (Scientific Volume Imaging (SVI), VB Hilversum, The Netherlands). Volume rendering of the stacks were performed with UCSF Chimera 1.10. 3D-Colocalisation analysis was performed with ImageJ (NIH, Bethesda, MD, USA) to determine Mander's 2 coefficient.

### Cell viability and apoptosis measurements

24 h after transfection in 10 cm dishes, cells were seeded in 96-wells plate at a density of 5,000 cells per well. Incubation with piceatannol, resveratrol, oligomycin, and DMSO was started 48 h after transfection and lasted for 36 h. Cell viability was measured using CellTiter-Blue assay (Promega) and apoptotic caspase activity via Caspase-Glo<sup>®</sup> 3/7 assay (Promega) following the standard protocols.

### Statistics

Data shown represent the mean  $\pm$  SEM. 'n' values refer to the number of individual experiments performed. EC<sub>50</sub> values are given as mean plus 95% confidential interval in parenthesis. For life cell imaging, numbers indicate the numbers of cells/independent repeats. If applicable analysis of variance (ANOVA) was used for data evaluation and statistical significance of differences between means was estimated by Bonferroni *post hoc* test or two-tailed Student's t-test assuming unequal variances, where applicable using GraphPad Prism 5.0f (GraphPad Software, La Jolla, CA, USA). The level of significance was defined as  $P < 0.05$ .

## Results

### Resveratrol and its derivative piceatannol cause apoptosis specifically in cancer cells

The effects of resveratrol and its derivate piceatannol on cell survival and apoptosis were compared in somatic short-cultured human umbilical vein endothelial cells (HUVEC) with the endothelial/epithelial cancer cell hybrid EA.hy926. Resveratrol and piceatannol had only a small effect on cell viability and caspase 3/7 activity in somatic HUVEC cells (Fig. 1A). In contrast, a 36 h treatment of the cancerous EA.hy926 cells with resveratrol or piceatannol decreased cell viability by more than 60 % and around 70%, respectively (Fig. 1A). Consistently, the activity of apoptotic caspases 3/7 upon treatment with either resveratrol or piceatannol remained unchanged in HUVEC while was increased by more than 7- and 8-fold in EA.hy926 cells (Fig. 1B).

Beside the endothelial-cancer hybrid cells (EA.hy926), resveratrol and piceatannol significantly decreased viability of the homo sapiens cervix adenocarcinoma cells (HeLa) by  $64.5 \pm 1.1$  (n = 3) and  $53.7 \pm 1.6\%$  (n = 3), respectively. In line with these findings, caspase 3/7 activity of HeLa cells incubated for 36 h with either 100  $\mu$ M resveratrol or 100  $\mu$ M piceatannol was increased app. 2.5-(n = 3) and 2.5-fold (n = 3), respectively.

Since resveratrol and piceatannol were reported to block the F1 subunit activity of mitochondrial ATP-synthase [17, 55, 56], we next tested whether the polyphenols' effect on cancer cell viability is due to their inhibitory effect on mitochondrial ATP synthase. Therefore, the effect of the ATP synthase inhibitor oligomycin A on cancer cell viability and

apoptosis was tested. Similar to resveratrol and piceatannol, oligomycin A (10  $\mu\text{M}$ ) reduced viability of EA.hy926 (Fig. 1A) and HeLa cells by  $74.6 \pm 7.6$  ( $n = 3$ ) and  $74.3 \pm 4.8\%$  ( $n = 3$ ), respectively. Likewise, in agreement to previous reports obtained in HepG2 cells [57] as well as in breast-, pancreatic-, and lung-cancer cells [58], oligomycin A enhanced caspase activity in EA.hy926 (Fig. 1B) and HeLa cells ( $n = 3$ ) by more than 10- and 3.7-fold, respectively.

In line with the other two ATP-synthase inhibitors described above (i.e. resveratrol, piceatannol), oligomycin A had no effect on cell viability (Fig. 1A) and the activity of caspases 3/7 of short-termed cultured HUVECs (Fig. 1B).

### **Resveratrol and its derivative piceatannol affect mitochondrial $\text{Ca}^{2+}$ uptake exclusively in cancer cells**

Because mitochondrial  $\text{Ca}^{2+}$  overload is known to represent a hallmark in the initiation of apoptotic caspase activity, we investigated the effect of the polyphenols and that of oligomycin A on mitochondrial  $\text{Ca}^{2+}$  uptake. After incubation with resveratrol, piceatannol, or oligomycin A mitochondrial  $\text{Ca}^{2+}$  uptake in response to  $\text{IP}_3$ -generating agonists was strongly increased in the cancerous cell lines (Fig. 2A, B). In contrast, resveratrol, piceatannol, or oligomycin A had much less or no effect on mitochondrial  $\text{Ca}^{2+}$  uptake to intracellular  $\text{Ca}^{2+}$  release in short-term cultured HUVECs (Fig. 2C).

The concentration response correlation for the effect of resveratrol on histamine-triggered mitochondrial  $\text{Ca}^{2+}$  uptake in EA.hy926 cells revealed an  $\text{EC}_{50}$  of 49.5 (29.9-84.8)  $\mu\text{M}$  with an Hill slope of  $0.86 \pm 0.10$  and a maximal potentiation of  $221.5 \pm 5.3\%$  at 300  $\mu\text{M}$  ( $n = 3$ ) (Fig. 3).

### **The effects of Resveratrol and its derivative on mitochondrial $\text{Ca}^{2+}$ uptake are due to an enhanced ER-mitochondria coupling in cancer cells**

The inter-organelle  $\text{Ca}^{2+}$  crosstalk between the ER and mitochondria takes place in regions of MAMs [59] and establishes the  $\text{Ca}^{2+}$  control on mitochondrial ATP production [60, 61]. On the other hand, the correct distance between ER and mitochondria is of crucial importance and, if the two organelles are too closely connected, the risk of uncontrolled mitochondrial  $\text{Ca}^{2+}$  overload yielding initiation of apoptosis occurs [62, 63]. In order to seek differences in the organization of mitochondrial  $\text{Ca}^{2+}$  handling between cancer and non cancer cells as basis of their opposite sensitivity to resveratrol, we investigated the MAM structure of EA.hy926 in comparison to short-term cultured HUVEC cells. Super-high resolution structural illumination microscopy revealed strongly increased ER-mitochondria contact in EA.hy926 compared to HUVECs (Fig. 4A & B). To clarify whether or not the effect of resveratrol and piceatannol on mitochondrial  $\text{Ca}^{2+}$  uptake in EA.hy926 and HeLa cells is indeed due to the enhanced stability of MAMs, we overexpressed mAKAP-RFP-CAAX construct that artificially tethers mitochondria to the plasma membrane, thus, disrupts the connection between ER and mitochondria (Fig. 4C & D). Destabilization of contact sites between ER and mitochondria by overexpression of mAKAP-RFP-CAAX caused a loss of the effect of resveratrol, piceatannol, and oligomycin A on the mitochondrial  $\text{Ca}^{2+}$  uptake in response to intracellular  $\text{Ca}^{2+}$  release in EA.hy926 (Fig. 4E)

and HeLa cells (Fig. 4F). These data indicate that the effect of the ATP synthase inhibitors on mitochondrial  $\text{Ca}^{2+}$  uptake in cancer cells relates to the inter-organelle  $\text{Ca}^{2+}$  organization between the mitochondria and the ER.

### **Resveratrol, piceatannol, and oligomycin A predominantly affect mitochondrial over cytosolic ATP levels**

Because resveratrol, piceatannol, and oligomycin A showed similar results in cell viability and mitochondrial  $\text{Ca}^{2+}$  uptake experiments, we next compared their effect on mitochondrial and cytosolic/global ATP levels. Measuring cytosolic and mitochondrial ATP by respectively-targeted fluorescence ATP probes [27, 64] revealed for all ATP-synthase inhibitors a small reduction in the cytosolic ATP level of app. 20% of the decrease observed by the combined addition of 2-deoxy-D-glucose and oligomycin A (Fig. 5A). In contrast, resveratrol, piceatannol, and oligomycin A strongly affected mitochondrial ATP levels of more than 50% of the decrease obtained by the addition of 2-deoxy-D-glucose and oligomycin A (Fig. 5B). These data indicate that three compounds, in the concentration used in this study (resveratrol 100  $\mu\text{M}$ , piceatannol 100  $\mu\text{M}$ , oligomycin A 10  $\mu\text{M}$ ), exhibited similar inhibitory potential and predominantly affected mitochondrial ATP levels while their effect for lowering global ATP was very small.

### **Drop of mitochondrial ATP influences SERCA activity in the MAMs yielding increased mitochondrial $\text{Ca}^{2+}$ sequestration**

Our data described above indicate that cancer cells establish an enforced ER-mitochondria coupling and are highly susceptible to resveratrol, piceatannol and oligomycin A that enhance mitochondrial  $\text{Ca}^{2+}$  sequestration specifically in cancer cells. Considering the importance of SERCA activity for the control of the  $\text{Ca}^{2+}$  concentration within the MAMs, we speculate that the inhibition of mitochondrial ATP-synthase may affect the activity of SERCA activity within the MAMs and, thus, hamper  $\text{Ca}^{2+}$  reuptake into the ER yielding increased mitochondrial  $\text{Ca}^{2+}$  sequestration. Therefore, the impact of resveratrol, piceatannol, and oligomycin A on SERCA activity was assessed by measuring the kinetics of ER  $\text{Ca}^{2+}$  refilling of previously depleted ER. All ATP-synthase inhibitors reduced ER  $\text{Ca}^{2+}$  uptake kinetic indicated as slope of ER refilling by about 70% (Fig. 6A&C).

To challenge our hypothesis that resveratrol, piceatannol, and oligomycin A affect SERCA activity by decreasing ATP within the ER-mitochondria junction, MAMs were disrupted by expressing mAKAP-RFP-CAAX construct that fixes mitochondria at the inner plasma membrane [65]. In cells with disrupted MAMs, the ATPase inhibitors failed to affect SERCA activity (Fig. 6B&C), thus, demonstrating that the close connection between ER and mitochondria is prerequisite for the effect of polyphenols to affect SERCA activity.

### **SERCA inhibition by resveratrol or piceatannol redirects the route of ER $\text{Ca}^{2+}$ into the mitochondria**

In HeLa cells, mitochondrial  $\text{Ca}^{2+}$  uptake is sensitive to a knock-down of MCU and UCP2/3 but not Letm1 (Fig. 7A). An inhibition of SERCA is known to impact mitochondrial  $\text{Ca}^{2+}$  uptake and to shift mitochondrial  $\text{Ca}^{2+}$  uptake route to become UCP2/3-independent but Letm1-dependent [66]. Accordingly, we next tested whether the redirection of the

mitochondrial  $\text{Ca}^{2+}$  uptake route also occurs by incubation with resveratrol, piceatannol, and oligomycin A as consequence of their inhibition of SERCA due to the inhibition of ATP-synthase by these compounds. In line with the reported effect of thapsigargin, all three ATP-synthase inhibitors abolished the contribution of UCP2/3 to mitochondrial  $\text{Ca}^{2+}$  uptake of intracellularly released  $\text{Ca}^{2+}$  (Fig. 7B). Hence, under condition of an inhibition of the altered mitochondrial  $\text{Ca}^{2+}$  uptake route by a depletion of Letm1 with respective siRNA resveratrol, piceatannol, and oligomycin A failed to enhance mitochondrial  $\text{Ca}^{2+}$  sequestration (Fig. 7C) that entirely depended on the core mitochondrial  $\text{Ca}^{2+}$  uniporter protein MCU under all conditions (Fig. 7D). These data indicate that thapsigargin as well as the ATP-synthase inhibitors resveratrol, piceatannol, and oligomycin A shift the MCU-established mitochondrial  $\text{Ca}^{2+}$  uptake from UCP2-dependent to an UCP2/3-independent but Letm1-dependent route.

### **Cancer cell death by resveratrol and piceatannol is dependent on mitochondrial $\text{Ca}^{2+}$ uptake**

Next we investigated whether or not resveratrol-, piceatannol-, or oligomycin A-triggered cancer cell death is due to increased mitochondrial  $\text{Ca}^{2+}$  uptake as a consequence of reduced SERCA activity due to the inhibition of mitochondrial ATP-synthase. Therefore, the effects of these ATP-synthase inhibitors on cell viability and the activity of the apoptotic pathway were tested in cancer cells (HeLa) depleted from the above verified two mitochondrial  $\text{Ca}^{2+}$  transporters involved in mitochondrial  $\text{Ca}^{2+}$  uptake under conditions of hampered SERCA activity due to ATP depletion, MCU and Letm1. Diminution of mitochondrial  $\text{Ca}^{2+}$  uptake by transfection with specific siRNAs against MCU and Letm1 rescued HeLa cells from initiation of apoptotic pathways (Fig. 8A) and reduced cell viability (Fig. 8B) in response to treatment with either resveratrol, piceatannol, or oligomycin A.

## **Discussion and Conclusions**

It is well documented that resveratrol and its derivate piceatannol induce cell death exclusively in cancer cells, including human breast cancer cell line MCF-7 [67, 68], human oral cancer cells OC2 [69], human promyelocytic leukemia cells HL-60 [70], human prostate carcinoma cells LNCaP, and HeLa cells [58]. In line with these reports, in the present work the hybrid-cell line EA.hy926 [71] and HeLa [72] were found to be sensitive to resveratrol- and piceatannol-induced cell death as well. In contrast to the endothelial hybrid-cell line EA.hy926, short term cultured endothelial cells were insensitive to resveratrol and piceatannol, thus, supporting the concept that these polyphenols specifically trigger cancer cell death but not that of respective somatic cells. Hence, resveratrol- and piceatannol-induced strong caspase 3/7 activity, indicating the initiation of the apoptotic pathways in cancer cells. The underlying reason(s) of the cancer cell specificity remains elusive. In fact, several mechanisms obviously involved in resveratrol-induced cell death have been solidly described but at the first glance it is not clear why an inhibition of ATP formation [15] [16, 17], ROS formation [18, 19], dissipation of mitochondrial membrane potential [13], or  $\text{Ca}^{2+}$  release from the endoplasmic reticulum (ER) [22] should be an option to trigger specifically cancer cell death and not that of somatic cells. However, resveratrol, instead of triggering cell death in somatic cells, counteracts pathological phenomena like cellular senescence [8]

and inflammation [7]. Therefore, we hypothesize that the polyphenols' cytotoxic effect on cancer cells depends on cancer cell-specific settings and, thus, intended to reveal such mechanisms within this work.

Mitochondrial  $\text{Ca}^{2+}$  overload is a hallmark of the initiation process of the apoptotic cell death pathway [73]. Our findings that resveratrol and piceatannol do not exhibit a direct effect on basal mitochondrial  $\text{Ca}^{2+}$  levels while they strongly augment mitochondrial  $\text{Ca}^{2+}$  uptake upon intracellular  $\text{Ca}^{2+}$  release in cancer cells (EA.hy926 and HeLa) but not in the somatic HUVEC cells, indicate that the action of the polyphenols is due to their modulatory effect on a cancer-specific setting in the  $\text{Ca}^{2+}$  link between the ER and the mitochondria. While the concentrations of the polyphenols used in this study are rather high, the concentration response relationship for mitochondrial  $\text{Ca}^{2+}$  uptake matches that reported on cancer cell death [10–13] and plasma levels found upon resveratrol treatment *in vivo* [74, 75].

Notably, a comparative analysis of the density of mitochondria-ER junctions (i.e. MAMs) in cancer and somatic cells using super-resolution microscopy revealed more inter-organelle junctions in cancer cell lines. These findings are in line with the recent report highlighting the importance of the ER-mitochondrial  $\text{Ca}^{2+}$  transfer in cancer cells [26] to boost mitochondrial ATP production that, in turn, meets the strongly elevated ATP demand of the ER in cancer [24, 25].

Our findings that a disruption of this tight mitochondria-ER coupling by fixing mitochondria at the inner side of the plasma membrane [65] prevented resveratrol/piceatannol-induced enhancement of mitochondrial  $\text{Ca}^{2+}$  uptake upon intracellular  $\text{Ca}^{2+}$  release, supports our concept that the polyphenols trigger cancer cell death by acting within the cancer-specific enforced mitochondria-ER junctions. Hence, these data indicate that resveratrol and piceatannol do not affect mitochondrial  $\text{Ca}^{2+}$  uptake *per se* but may foster inter-organelle  $\text{Ca}^{2+}$  flux. Notably, the inter-organelle  $\text{Ca}^{2+}$  transfer between the ER to the mitochondria mainly depends on the amount of intracellularly released  $\text{Ca}^{2+}$ , the mitochondrial  $\text{Ca}^{2+}$  uptake machinery and the amount of  $\text{Ca}^{2+}$  re-sequestration from the MAM back into the ER by SERCA [54, 66]. While the first two mechanisms appeared to be unaffected by resveratrol or piceatannol, a modulation of SERCA activity by these polyphenols appears likely due to their great inhibitory effect on mitochondrial ATP formation. Hence, our data revealed that resveratrol and piceatannol only marginally affected cytosolic ATP levels, while their impact on mitochondrial ATP content was strong and comparable with the known ATP synthase inhibitor oligomycin A that is known to cause a slight drop in cytosolic [76] and a massive drop in mitochondrial ATP levels [77].

Remarkably, oligomycin A, that mimics the impact of resveratrol and piceatannol on mitochondrial ATP formation, exhibited identical effects on specific cancer cell death and mitochondrial  $\text{Ca}^{2+}$  uptake, thus, indicating that the decrease in mitochondrial ATP formation is the reason for cancer cell death induced by resveratrol and piceatannol (and oligomycin A). This conclusion is further supported by our findings that resveratrol, piceatannol and oligomycin A clearly affect SERCA-mediated  $\text{Ca}^{2+}$  sequestration into the ER in HeLa cells while no effect on ER depletion was found. Importantly, a disruption of the

tight mitochondria-ER coupling by fixing mitochondria at the inner side of the plasma membrane abolished the inhibitory effect of the polyphenols and oligomycin A on SERCA-mediated ER  $\text{Ca}^{2+}$  refilling. These data suggest that the inhibition of mitochondrial ATP formation yields reduced SERCA activity within the cancer cell-specific enforced mitochondria-ER coupling.

Inhibition of SERCA activity was shown to shift mitochondrial  $\text{Ca}^{2+}$  uptake routes from an UCP2/3-dependent and Letm1-independent towards an UCP2/3-independent and Letm1-dependent pathway [66]. In line with this report, our findings reported herein demonstrate that the ATPase inhibitors yielded loss of UCP2/3-dependency but the engagement of Letm1 in MCU-dependent mitochondrial  $\text{Ca}^{2+}$  uptake as a consequence of the reduction of SERCA activity due to the lack of local ATP supply. Notably, because SERCA activity counteracts the inter-organelle  $\text{Ca}^{2+}$  transfer from the ER to the mitochondria its inhibition by the lack of ATP due to the inhibition of ATP synthase by resveratrol, piceatannol, or oligomycin A yields enhanced mitochondrial  $\text{Ca}^{2+}$  accumulation. Hence, our findings that the siRNA-mediated knock-down of MCU and Letm1 prevented resveratrol-, piceatannol-, and oligomycin A-triggered initiation of the apoptotic pathway and cancer cell death, support our hypothesis of an enhanced mitochondrial  $\text{Ca}^{2+}$  sequestration within the enforced ER-mitochondria coupling in cancer cells as molecular mechanisms of resveratrol- and piceatannol-induced cancer cell death.

Our data presented herein demonstrate that the inhibition of ATP synthase by resveratrol, piceatannol, or oligomycin A specifically affect the tight inter-organelle coupling of mitochondria and ER in cancer cells, yielding enhanced mitochondrial  $\text{Ca}^{2+}$  accumulation, the initiation of apoptotic pathways, and, ultimately, cancer cell death (Fig. 9).

## Acknowledgements

We thank Dr. Nicole A. Hofmann, Institut of Experimental and Clinical Pharmacology, Medical University of Graz, Austria and Prof. Dr. Dirk Strunk, Experimental and Clinical Cell Therapy Institute, Paracelsus, Medical University of Salzburg, Austria for kindly providing the short-term cultured HUVECs, Dr. C.J.S. Edgell (University of North Carolina, Chapel Hill, NC) for the EA.hy926 cells, and Prof. Dr. György Hajnóczy (Thomas Jefferson University, Philadelphia, Pennsylvania, USA) for kindly providing us the AKAP-RFP-CAAX construct. C.T.M. and C.K. are fellows of the Doctoral College “Metabolic and Cardiovascular Disease” (FWF W1226-B18) and were funded by the Medical University of Graz. BG and this work are funded by the FWF (W 1226-B18, DKplus Metabolic and Cardiovascular Disease) and P 28529-B27. W.P. was a fellow from the Austrian academic exchange service (ÖAD). Microscopic equipment is part of the NIKON-Center of Excellence, Graz that is supported by Nikon, Inc. (Austria, Netherlands, Japan), BioTechMed Graz and the Federal Ministry of Science, Research and Economy in course of the HSRM 2013 initiative.

## Abbreviations

<b>EA.hy926</b>	hybridoma cell line of primary human umbilical vein cells fused with the adeno-carcinomic human alveolar basal epithelial (human lung cancer) cell A549
<b>EMRE</b>	essential MCU regulator
<b>ER</b>	endoplasmic reticulum
<b>GRP75</b>	glucose-regulated protein 75

<b>HeLa</b>	homo sapiens cervix adenocarcinoma cells
<b>HUVEC</b>	human umbilical vein endothelial cells
<b>Letm1</b>	leucine zipper/EF-hand-containing trans-membrane domain 1
<b>MCU</b>	mitochondrial calcium uniporter
<b>Mfn-2</b>	mitofusin 2
<b>MICU1</b>	mitochondrial calcium uptake 1
<b>MICU2</b>	mitochondrial calcium uptake 2
<b>MCUR1</b>	MCU regulator protein 1
<b>NCLX</b>	mitochondrial Na <sup>+</sup> /Ca <sup>2+</sup> exchanger
<b>PACS2</b>	phosphofurin acidic cluster sorting protein 2
<b>SERCA</b>	sarco/endoplasmic reticulum Ca <sup>2+</sup> ATPase
<b>SIM</b>	structural illumination microscopy
<b>UCP2/3</b>	uncoupling protein 2 and 3

## References

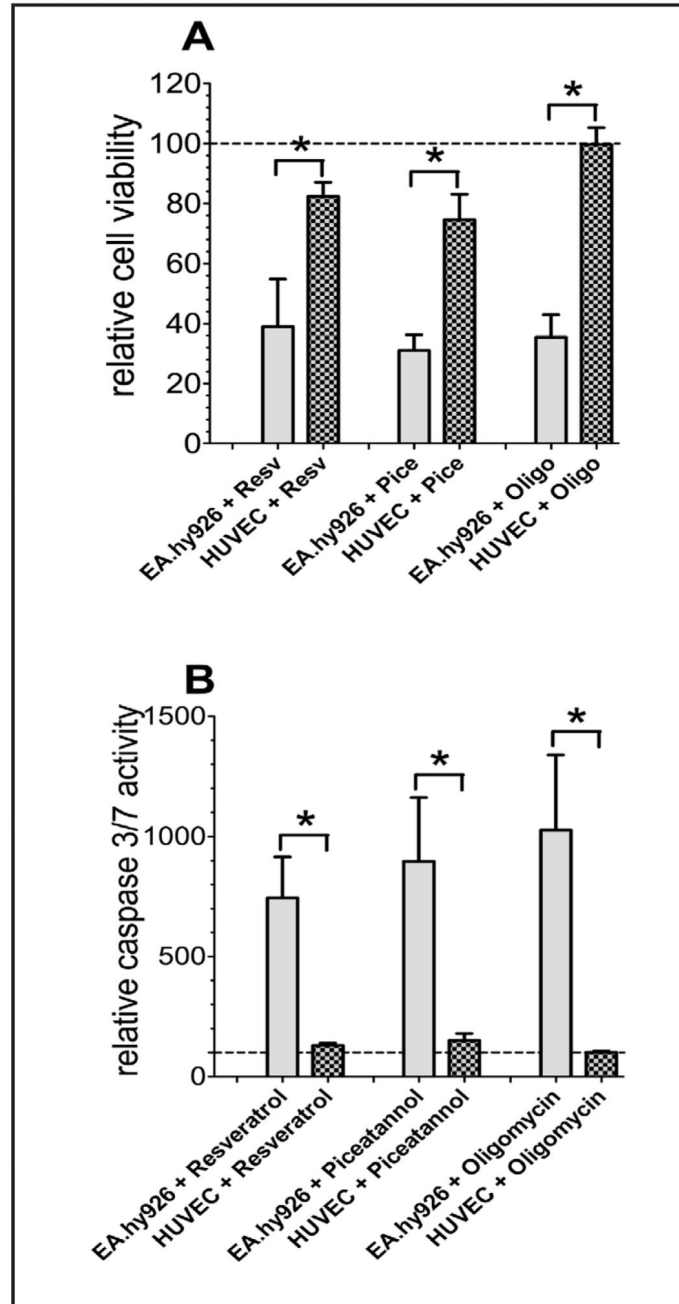
1. Bavaresco L, Lucini L, Busconi M, Flamini R, De Rosso M. Wine Resveratrol: From the Ground Up. *Nutrients*. 2016; 8:222. [PubMed: 27089363]
2. Varoni EM, Faro Lo AF, Sharifi-Rad J, Iriti M. Anticancer Molecular Mechanisms of Resveratrol. *Front Nutr*. 2016; 3:8. [PubMed: 27148534]
3. Gehm BD, McAndrews JM, Chien PY, Jameson JL. Resveratrol, a polyphenolic compound found in grapes and wine, is an agonist for the estrogen receptor. *Proc Natl Acad Sci USA*. 1997; 94:14138–14143. [PubMed: 9391166]
4. Chang LW, Juang LJ, Wang BS, Wang MY, Tai HM, Hung WJ, Chen YJ, Huang MH. Antioxidant and antityrosinase activity of mulberry (*Morus alba* L.) twigs and root bark. *Food Chem Toxicol*. 2011; 49:785–790. [PubMed: 21130832]
5. Shrikanta A, Kumar A, Govindaswamy V. Resveratrol content and antioxidant properties of underutilized fruits. *J Food Sci Technol*. 2015; 52:383–390. [PubMed: 25593373]
6. Das A, Banik NL, Ray SK. Flavonoids activated caspases for apoptosis in human glioblastoma T98G and U87MG cells but not in human normal astrocytes. *Cancer*. 2010; 116:164–176. [PubMed: 19894226]
7. Bereswill S, Munoz M, Fischer A, Plickert R, Haag LM, Otto B, Kühl AA, Loddenkemper C, Göbel UB, Heimesaat MM. Anti-inflammatory effects of resveratrol, curcumin and simvastatin in acute small intestinal inflammation. *PLoS ONE*. 2010; 5:e15099. [PubMed: 21151942]
8. McCalley AE, Kaja S, Payne AJ, Koulen P. Resveratrol and Calcium Signaling: Molecular Mechanisms and Clinical Relevance. *Molecules*. 2014; 19:7327–7340. [PubMed: 24905603]
9. Piotrowska H, Kucinska M, Murias M. Biological activity of piceatannol: Leaving the shadow of resveratrol. *Mutat Res*. 2012; 750:60–82. [PubMed: 22108298]
10. Tinhofer I, Bernhard D, Senfter M, Anether G, Loeffler M, Kroemer G, Kofler R, Csordas A, Greil R. Resveratrol, a tumor-suppressive compound from grapes, induces apoptosis via a novel mitochondrial pathway controlled by Bcl-2. *FASEB J*. 2001; 15:1613–1615. [PubMed: 11427503]

11. Rojas C, Pan-Castillo B, Valls C, Pujadas G, Garcia-Vallve S, Arola L, Mulero M. Resveratrol Enhances Palmitate-Induced ER Stress and Apoptosis in Cancer Cells. *PLoS ONE*. 2014; 9:e113929. [PubMed: 25436452]
12. Qin Y, Ma Z, Dang X, Le W, Ma Q. Effect of resveratrol on proliferation and apoptosis of human pancreatic cancer MIA PaCa-2 cells may involve inhibition of the Hedgehog signaling pathway. *Mol Med Rep*. 2014; 10:2563–2567. [PubMed: 25190613]
13. Sareen D, Darjatmoko SR, Albert DM, Polans AS. Mitochondria, calcium, and calpain are key mediators of resveratrol-induced apoptosis in breast cancer. *Mol Pharmacol*. 2007; 72:1466–1475. [PubMed: 17848600]
14. Nie P, Hu W, Zhang T, Yang Y, Hou B, Zou Z. Synergistic Induction of Erlotinib-Mediated Apoptosis by Resveratrol in Human Non-Small-Cell Lung Cancer Cells by Down-Regulating Survivin and Up-Regulating PUMA. *Cell Physiol Biochem*. 2015; 35:2255–2271. [PubMed: 25895606]
15. Zini R, Morin C, Bertelli A, Bertelli A, Tillement JP. Effects of resveratrol on the rat brain respiratory chain. *Drugs Exp Clin Res*. 1999; 25:87–97. [PubMed: 10370869]
16. Dadi PK, Ahmad M, Ahmad Z. Inhibition of ATPase activity of Escherichia coli ATP synthase by polyphenols. *Int J Biol Macromol*. 2009; 45:72–79. [PubMed: 19375450]
17. Gledhill JR, Walker JE. Inhibition sites in F1-ATPase from bovine heart mitochondria. *Biochem J*. 2005; 386:591–598. [PubMed: 15537385]
18. Sassi N, Mattarei A, Azzolini M, Szabò I, Paradisi C, Zoratti M, Biasutto L. Cytotoxicity of mitochondria-targeted resveratrol derivatives: interactions with respiratory chain complexes and ATP synthase. *Biochim Biophys Acta*. 2014; 1837:1781–1789. [PubMed: 24997425]
19. Santandreu FM, Valle A, Oliver J, Roca P. Resveratrol Potentiates the Cytotoxic Oxidative Stress Induced by Chemotherapy in Human Colon Cancer Cells. *Cell Physiol Biochem*. 2011; 28:219–228. [PubMed: 21865729]
20. Wang R, Liu Y, Liu X, Jia S, Zhao J, Cui D, Wang L. Resveratrol Protects Neurons and the Myocardium by Reducing Oxidative Stress and Ameliorating Mitochondria Damage in a Cerebral Ischemia Rat Model. *Cell Physiol Biochem*. 2014; 34:854–864. [PubMed: 25199673]
21. Guo R, Su Y, Liu B, Li S, Zhou S, Xu Y. Resveratrol Suppresses Oxidised Low-Density Lipoprotein-Induced Macrophage Apoptosis through Inhibition of Intracellular Reactive Oxygen Species Generation, LOX-1, and the p38 MAPK Pathway. *Cell Physiol Biochem*. 2014; 34:603–616. [PubMed: 25116358]
22. Mahyar-Roemer M, Katsen A, Mestres P, Roemer K. Resveratrol induces colon tumor cell apoptosis independently of p53 and preceded by epithelial differentiation, mitochondrial proliferation and membrane potential collapse. *Int J Cancer*. 2001; 94:615–622. [PubMed: 11745454]
23. Delmas D, Lancon A, Colin D, Jannin B, Latruffe N. Resveratrol as a chemopreventive agent: A promising molecule for fighting cancer. *Curr Drug Targets*. 2006; 7:423–442. [PubMed: 16611030]
24. Wang W-A, Groenendyk J, Michalak M. Endoplasmic reticulum stress associated responses in cancer. *Biochim Biophys Acta*. 2014; 1843:2143–2149. [PubMed: 24440276]
25. Dolfi SC, Chan LL-Y, Qiu J, Tedeschi PM, Bertino JR, Hirshfield KM, Oltvai ZN, Vazquez A. The metabolic demands of cancer cells are coupled to their size and protein synthesis rates. *Cancer Metab*. 2013; 1:20. [PubMed: 24279929]
26. Cárdenas C, Müller M, McNeal A, Lovy A, Ja a F, Bustos G, Urrea F, Smith N, Molgó J, Diehl JA, Ridky TW, et al. Selective Vulnerability of Cancer Cells by Inhibition of Ca<sup>2+</sup> Transfer from Endoplasmic Reticulum to Mitochondria. *Cell Rep*. 2016; 14:2313–2324. [PubMed: 26947070]
27. Vishnu N, Jadoon Khan M, Karsten F, Groschner LN, Waldeck-Weiermair M, Rost R, Hallström S, Imamura H, Graier WF, Malli R. ATP increases within the lumen of the endoplasmic reticulum upon intracellular Ca<sup>2+</sup> release. *Mol Biol Cell*. 2014; 25:368–379. [PubMed: 24307679]
28. Denton RM. Regulation of mitochondrial dehydrogenases by calcium ions. *Biochim Biophys Acta*. 2009; 1787:1309–1316. [PubMed: 19413950]
29. Gerencser AA, Chinopoulos C, Birket MJ, Jastroch M, Vitelli C, Nicholls DG, Brand M. Quantitative measurement of mitochondrial membrane potential in cultured cells: calcium-induced

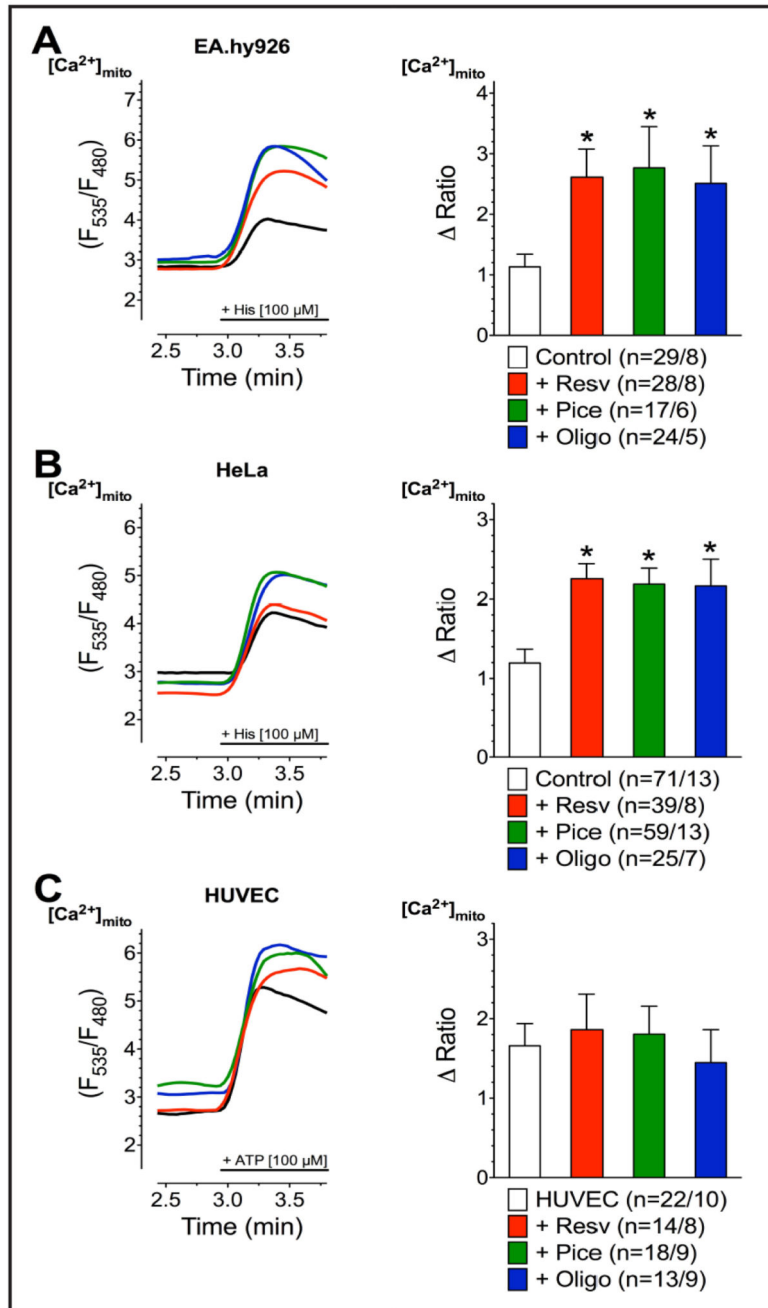
- de- and hyperpolarization of neuronal mitochondria. *J Physiol (Lond)*. 2012; 590:2845–2871. [PubMed: 22495585]
30. Malli R, Frieden M, Osibow K, Graier WF. Mitochondria efficiently buffer subplasmalemmal  $\text{Ca}^{2+}$  elevation during agonist stimulation. *J Biol Chem*. 2003; 278:10807–10815. [PubMed: 12529366]
  31. Hajnóczky G, Csordás G, Das S, Garcia-Perez C, Saotome M, Sinha Roy S, eYi M. Mitochondrial calcium signalling and cell death: approaches for assessing the role of mitochondrial  $\text{Ca}^{2+}$  uptake in apoptosis. *Cell Calcium*. 2006; 40:553–560. [PubMed: 17074387]
  32. Pizzo P, Drago I, Filadi R, Pozzan T. Mitochondrial  $\text{Ca}^{2+}$  homeostasis: mechanism, role, and tissue specificities. *Pflugers Arch*. 2012; 464:3–17. [PubMed: 22706634]
  33. Waldeck-Weiermair M, Alam MR, Khan MJ, Deak AT, Vishnu N, Karsten F, Imamura H, Graier WF, Malli R. Spatiotemporal correlations between cytosolic and mitochondrial  $\text{Ca}^{2+}$  signals using a novel red-shifted mitochondrial targeted cameleon. *PLoS ONE*. 2012; 7:e45917. [PubMed: 23029314]
  34. Giacomello M, Drago I, Bortolozzi M, Scorzeto M, Gianelle A, Pizzo P, Pozzan T.  $\text{Ca}^{2+}$  hot spots on the mitochondrial surface are generated by  $\text{Ca}^{2+}$  mobilization from stores, but not by activation of store-operated  $\text{Ca}^{2+}$  channels. *Mol Cell*. 2010; 38:280–290. [PubMed: 20417605]
  35. Vance JE. Phospholipid synthesis in a membrane fraction associated with mitochondria. *J Biol Chem*. 1990; 265:7248–7256. [PubMed: 2332429]
  36. Merkwirth C, Langer T. Mitofusin 2 builds a bridge between ER and mitochondria. *Cell*. 2008; 135:1165–1167. [PubMed: 19109886]
  37. de Brito OM, Scorrano L. Mitofusin 2 tethers endoplasmic reticulum to mitochondria. *Nature*. 2008; 456:605–610. [PubMed: 19052620]
  38. Szabadkai G, Bianchi K, Várnai P, De Stefani D, Wieckowski MR, Cavagna D, Nagy A, Balla T, Rizzuto R. Chaperone-mediated coupling of endoplasmic reticulum and mitochondrial  $\text{Ca}^{2+}$  channels. *J Cell Biol*. 2006 Dec 18; 175:901–911. [PubMed: 17178908]
  39. Simmen T, Aslan JE, Blagoveshchenskaya AD, Thomas L, Wan L, Xiang Y, Feliciangeli SF, Hung C-H, Crump CM, Thomas G. PACS-2 controls endoplasmic reticulum-mitochondria communication and Bid-mediated apoptosis. *EMBO J*. 2005; 24:717–729. [PubMed: 15692567]
  40. Kamer KJ, Mootha VK. The molecular era of the mitochondrial calcium uniporter. *Nat Rev Mol Cell Biol*. 2015; 16:545–553. [PubMed: 26285678]
  41. De Stefani D, Rizzuto R. Structure and function of the mitochondrial calcium uniporter complex. *Biochim Biophys Acta*. 2015; 1853:2006–2011. [PubMed: 25896525]
  42. Palty R, Silverman WF, Hershinkel M, Caporale T, Sensi SL, Parnis J, Nolte C, Fishman D, Shoshan-Barmatz V, Herrmann S, Khananshvilis D, et al. NCLX is an essential component of mitochondrial  $\text{Na}^+/\text{Ca}^{2+}$  exchange. *Proc Natl Acad Sci USA*. 2010; 107:436–441. [PubMed: 20018762]
  43. Baughman JM, Perocchi F, Girgis HS, Plovanich M, Belcher-Timme CA, Sancak Y, Bao XR, Strittmatter L, Goldberger O, Bogorad RL, Kotliansky V, et al. Integrative genomics identifies MCU as an essential component of the mitochondrial calcium uniporter. *Nature*. 2011; 476:341–345. [PubMed: 21685886]
  44. De Stefani D, Raffaello A, Teardo E, Szabò I, Rizzuto R. A forty-kilodalton protein of the inner membrane is the mitochondrial calcium uniporter. *Nature*. 2011; 476:336–340. [PubMed: 21685888]
  45. Raffaello A, De Stefani D, Sabbadin D, Teardo E, Merli G, Picard A, Checchetto V, Moro S, Szabò I, Rizzuto R. The mitochondrial calcium uniporter is a multimer that can include a dominant-negative pore-forming subunit. *EMBO J*. 2013; 32:2362–2376. [PubMed: 23900286]
  46. Sancak Y, Markhard AL, Kitami T, Kovács-Bogdán E, Kamer KJ, Udeshi ND, Carr SA, Chaudhuri D, Clapham DE, Li AA, Calvo SE, et al. EMRE is an essential component of the mitochondrial calcium uniporter complex. *Science*. 2013; 342:1379–1382. [PubMed: 24231807]
  47. Mallilankaraman K, Cárdenas C, Doonan PJ, Chandramoorthy HC, Irrinki KM, Golenár T, Csordás G, Madireddi P, Yang J, Müller M, Miller R, et al. MCUR1 is an essential component of mitochondrial  $\text{Ca}^{2+}$  uptake that regulates cellular metabolism. *Nat Cell Biol*. 2012; 14:1336–1343. [PubMed: 23178883]

48. Vais H, Tanis JE, Müller M, Payne R, Mallilankaraman K, Foskett JK. MCUR1, CCDC90A, Is a Regulator of the Mitochondrial Calcium Uniporter. *Cell Metab.* 2015; 22:533–535. [PubMed: 26445506]
49. Perocchi F, Gohil VM, Girgis HS, Bao XR, McCombs JE, Palmer AE, Mootha VK. MICU1 encodes a mitochondrial EF hand protein required for Ca<sup>2+</sup> uptake. *Nature.* 2010; 467:291–296. [PubMed: 20693986]
50. Plovanich M, Bogorad RL, Sancak Y, Kamer KJ, Strittmatter L, Li AA, et al. MICU2, a paralog of MICU1, resides within the mitochondrial uniporter complex to regulate calcium handling. *PLoS ONE.* 2013; 8:e55785. [PubMed: 23409044]
51. Csordás G, Golenár T, Seifert EL, Kamer KJ, Sancak Y, Perocchi F, Moffat C, Weaver D, de la Fuente Perez S, Bogorad R, Koteliansky V, et al. MICU1 Controls Both the Threshold and Cooperative Activation of the Mitochondrial Ca<sup>2+</sup> Uniporter. *Cell Metab.* 2013:976–987. [PubMed: 23747253]
52. Wang L, Yang X, Li S, Wang Z, Liu Y, Feng J, Zhu Y, Shen Y. Structural and mechanistic insights into MICU1 regulation of mitochondrial calcium uptake. *EMBO J.* 2014; 33:594–604. [PubMed: 24514027]
53. Waldeck-Weiermair M, Malli R, Parichatikanond W, Gottschalk B, Madreiter-Sokolowski CT, Klec C, Rost R, Graier WF. Rearrangement of MICU1 multimers for activation of MCU is solely controlled by cytosolic Ca<sup>2+</sup>. *Sci Rep.* 2015; 5:15602. [PubMed: 26489515]
54. De Marchi U, Castelbou C, Demaurex N. Uncoupling protein 3 (UCP3) modulates the activity of Sarco/endoplasmic reticulum Ca<sup>2+</sup>-ATPase (SERCA) by decreasing mitochondrial ATP production. *J Biol Chem.* 2011; 286:32533–32541. [PubMed: 21775425]
55. Zheng JB, Ramirez VD. Piceatannol, a stilbene phytochemical, inhibits mitochondrial F0F1-ATPase activity by targeting the F1 complex. *Biochem Biophys Res Commun.* 1999; 261:499–503. [PubMed: 10425214]
56. Zheng J, Ramirez VD. Inhibition of mitochondrial proton F0F1-ATPase/ATP synthase by polyphenolic phytochemicals. *Br J Pharmacol.* 2000; 130:115–1123.
57. Li YC, Fung KP, Kwok TT, Lee CY, Suen YK, Kong SK. Mitochondria-targeting drug oligomycin blocked P-glycoprotein activity and triggered apoptosis in doxorubicin-resistant HepG2 cells. *Chemotherapy.* 2004; 50:55–62. [PubMed: 15211078]
58. Palorini R, Simonetto T, Cirulli C, Chiaradonna F. Mitochondrial complex I inhibitors and forced oxidative phosphorylation synergize in inducing cancer cell death. *Int J Cell Biol.* 2013; 2013:243876. [PubMed: 23690779]
59. Raturi A, Simmen T. Where the endoplasmic reticulum and the mitochondrion tie the knot: the mitochondria-associated membrane (MAM). *Biochim Biophys Acta.* 2013; 1833:213–224. [PubMed: 22575682]
60. Nakano M, Imamura H, Nagai T, Noji H. Ca<sup>2+</sup> regulation of mitochondrial ATP synthesis visualized at the single cell level. *Acs Chem Biol.* 2011; 6:709–715. [PubMed: 21488691]
61. Tarasov AI, Griffiths EJ, Rutter GA. Regulation of ATP production by mitochondrial Ca<sup>2+</sup> Cell Calcium. 2012; 52:28–35. [PubMed: 22502861]
62. Pinton P, Giorgi C, Siviero R, Zecchini E, Rizzuto R. Calcium and apoptosis: ER-mitochondria Ca<sup>2+</sup> transfer in the control of apoptosis. *Oncogene.* 2008; 27:6407–6418. [PubMed: 18955969]
63. Bui M, Gilady SY, Fitzsimmons REB, Benson MD, Lynes EM, Gesson K, Alto NM, Strack S, Scott JD, Simmen T. Rab32 modulates apoptosis onset and mitochondria-associated membrane (MAM) properties. *J Biol Chem.* 2010; 285:31590–31602. [PubMed: 20670942]
64. Imamura H, Nhat KPH, Togawa H, Saito K, Iino R, Kato-Yamada Y, Nagai T, Noji H. Visualization of ATP levels inside single living cells with fluorescence resonance energy transfer-based genetically encoded indicators. *Proc Natl Acad Sci USA.* 2009; 106:15651–15656. [PubMed: 19720993]
65. Naghdi S, Waldeck-Weiermair M, Fertschai I, Poteser M, Graier WF, Malli R. Mitochondrial Ca<sup>2+</sup> uptake and not mitochondrial motility is required for STIM1-Orai1-dependent store-operated Ca<sup>2+</sup> entry. *J Cell Sci.* 2010; 123:2553–2564. [PubMed: 20587595]
66. Waldeck-Weiermair M, Deak AT, Groschner LN, Alam MR, Jean-Quartier C, Malli R, Graier WF. Molecularly Distinct Routes of Mitochondrial Ca<sup>2+</sup> Uptake Are Activated Depending on the

- Activity of the Sarco/Endoplasmic Reticulum  $\text{Ca}^{2+}$  ATPase (SERCA). *J Biol Chem.* 2013; 288:15367–15379. [PubMed: 23592775]
67. Venkatadri R, Muni T, Iyer AKV, Yakisich JS, Azad N. Role of apoptosis-related miRNAs in resveratrol-induced breast cancer cell death. *Cell Death Dis.* 2016; 7:e2104. [PubMed: 26890143]
  68. Gomez LS, Zancan P, Marcondes MC, Ramos-Santos L, Meyer-Fernandes JR, Sola-Penna M, Da Silva D. Resveratrol decreases breast cancer cell viability and glucose metabolism by inhibiting 6-phosphofructo-1-kinase. *Biochimie.* 2013; 95:1336–1343. [PubMed: 23454376]
  69. Chang H-J, Chou C-T, Chang H-T, Liang W-Z, Hung T-Y, Li YD, Fang Y, Kuo C, Kuo D, Shieh P, Jan CR. Mechanisms of resveratrol-induced changes in cytosolic free calcium ion concentrations and cell viability in OC2 human oral cancer cells. *Hum Exp Toxicol.* 2015; 34:289–299. [PubMed: 24925362]
  70. Surh Y-J, Hurh YJ, Kang JY, Lee E, Kong G, Lee SJ. Resveratrol, an antioxidant present in red wine, induces apoptosis in human promyelocytic leukemia (HL-60) cells. *Cancer Lett.* 1999; 140:1–10. [PubMed: 10403535]
  71. Edgell CJ, McDonald CC, Graham JB. Permanent cell line expressing human factor VIII-related antigen established by hybridization. *Proc Natl Acad Sci USA.* 1983; 80:3734–3737. [PubMed: 6407019]
  72. Scherer WF, Syverton JT, Gey GO. Studies on the propagation *in vitro* of poliomyelitis viruses. IV. Viral multiplication in a stable strain of human malignant epithelial cells (strain HeLa) derived from an epidermoid carcinoma of the cervix. *J Exp Med.* 1953; 97:695–710. [PubMed: 13052828]
  73. Nicotera P, Orrenius S. The role of calcium in apoptosis. *Cell Calcium.* 1998; 23:173–180. [PubMed: 9601613]
  74. Sale S, Verschoyle RD, Boocock D, Jones DJL, Wilsher N, Ruparelia KC, Potter GA, Farmer PB, Steward WP, Gescher AJ. Pharmacokinetics in mice and growth-inhibitory properties of the putative cancer chemopreventive agent resveratrol and the synthetic analogue trans 3,4,5,4'-tetramethoxystilbene. *Br J Cancer.* 2004 Feb 9;90:736–744. [PubMed: 14760392]
  75. Baur JA, Sinclair DA. Therapeutic potential of resveratrol: the *in vivo* evidence. *Nat Rev Drug Discov.* 2006; 5:493–506. [PubMed: 16732220]
  76. Huang H, Zhang X, Li S, Liu N, Lian W, McDowell E, Zhou P, Zhao C, Guo H, Zhang C, Yang C, et al. Physiological levels of ATP negatively regulate proteasome function. *Cell Res.* 2010; 20:1372–1385. [PubMed: 20805844]
  77. Brand MD, Nicholls DG. Assessing mitochondrial dysfunction in cells. *Biochem J.* 2011; 435:297–312. [PubMed: 21726199]

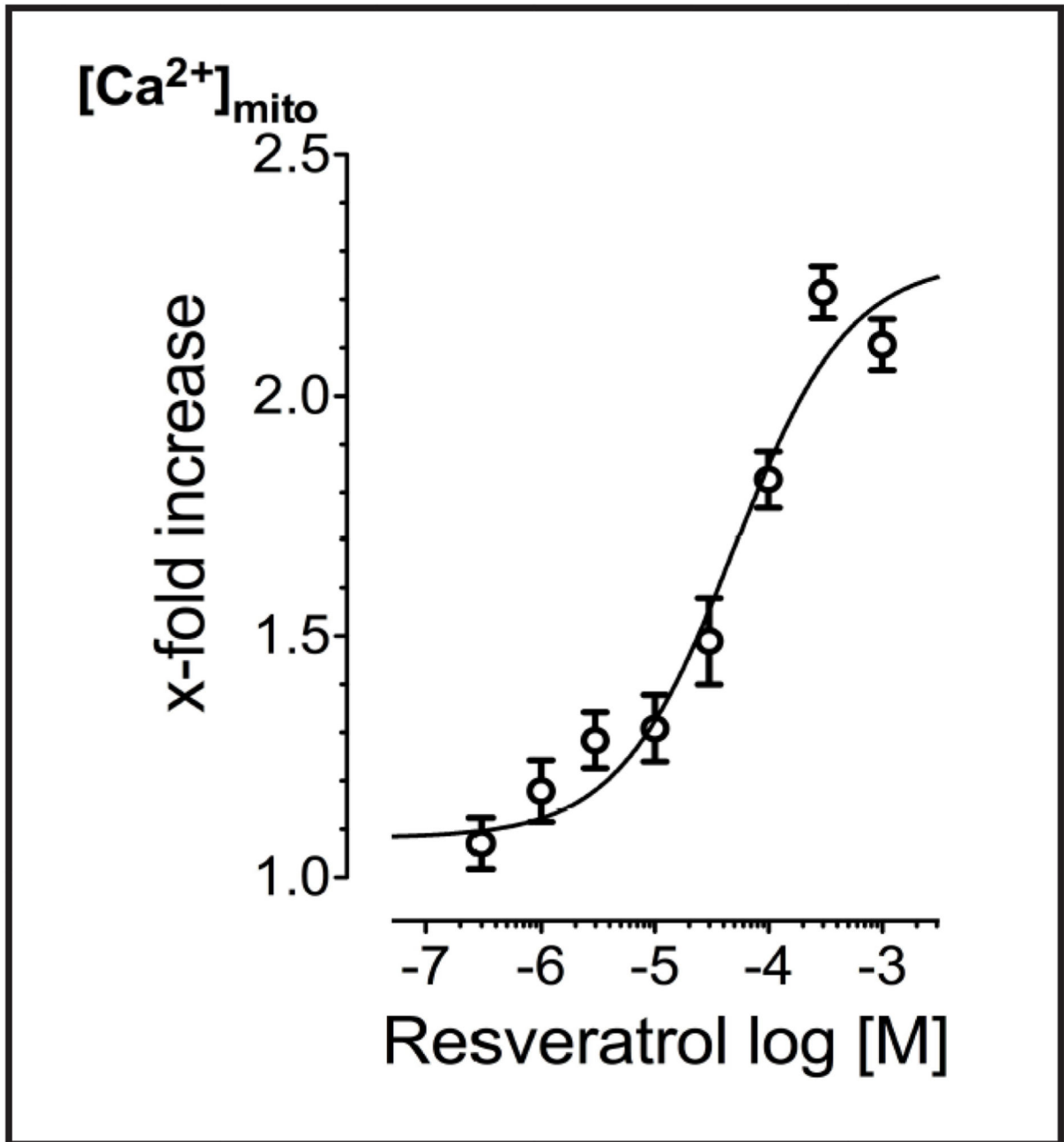


**Fig. 1.** Cell viability of EA.hy926 and HUVEC cells was measured via Celltiter-Blue assay according to the standard protocol after 36 h of incubation with resveratrol (Resv; 100  $\mu$ M), piceatannol (Pice, 100  $\mu$ M) or oligomycin A (oligo, 10  $\mu$ M) and calculated as percentage of viable cells normalized to control conditions (A). Caspase activity of EA.hy926 and HUVEC cells, normalized to control conditions as percentage of viable cells, was determined with Caspase 3/7-Glo assay following the standard protocol after 36 h of compound incubation (B).

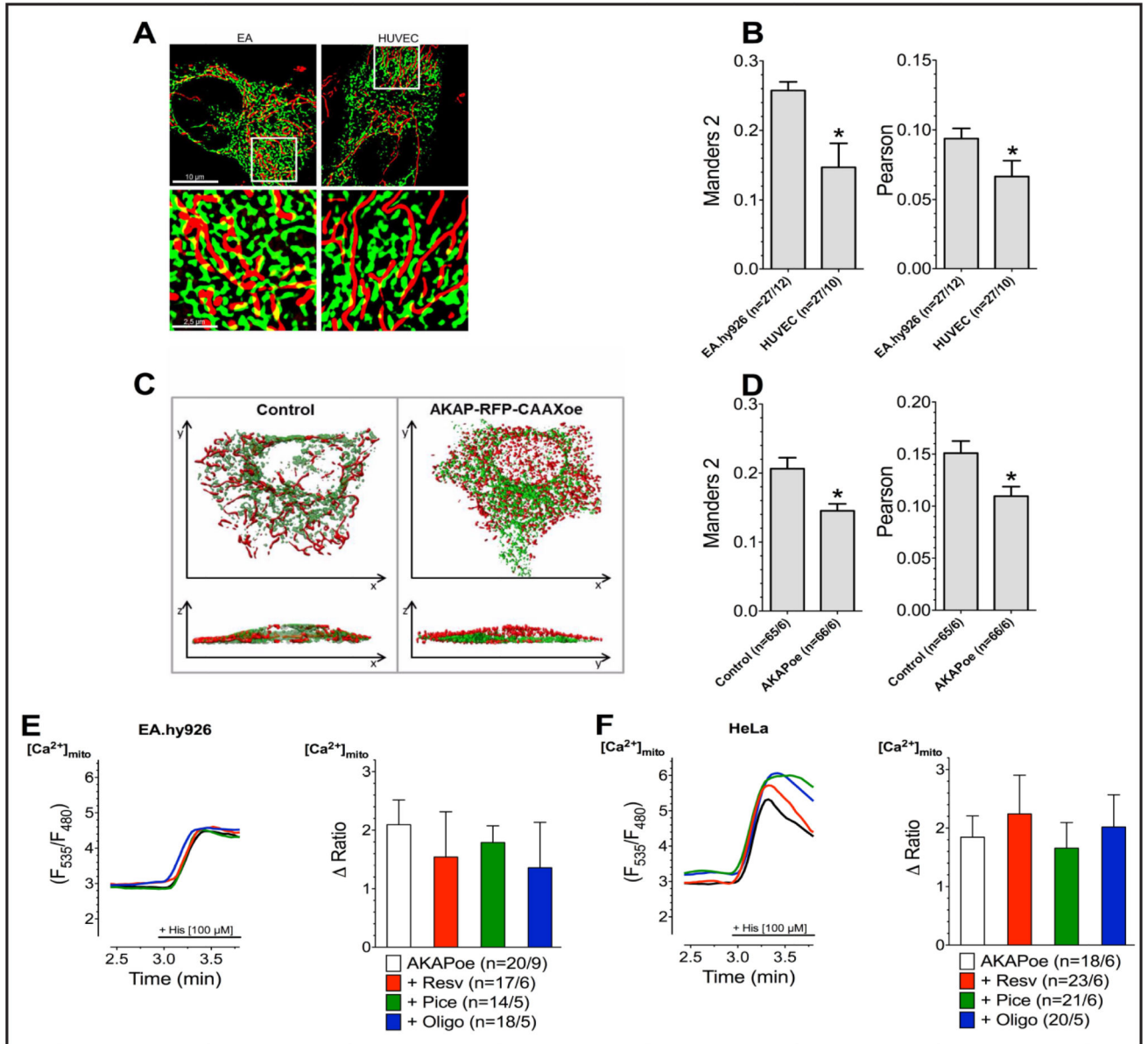


**Fig. 2.** Representative curves (left panels) reflect  $mtCa^{2+}$  ratio signals over time of EA.hy926 (A), HeLa (B), and HUVEC cells (C), expressing 4mtD3cpv, in response to  $IP_3$  generating agonists measured in  $Ca^{2+}$ -free solution under control conditions (black curve) as well as after 3 min incubations with 100  $\mu$ M resveratrol (red curve), 100  $\mu$ M piceatannol (green curve), or 10  $\mu$ M oligomycin A (blue curve). To induce  $Ca^{2+}$  release from intracellular ER, 100  $\mu$ M histamine (His) was applied to HeLa and Ea.hy926 cells, whereas 100  $\mu$ M ATP was used as an agonist for HUVEC cells. Bars (right panels) represent an average of maximal

ratio signals (mean  $\pm$  SEM) upon IP<sub>3</sub> generating agonist stimulation in Ca<sup>2+</sup>-free solution under control conditions (white columns; EA.hy926: n=29/8, HeLa: n=71/13, and HUVEC: n=22/10) as well as of cells treated with resveratrol (red columns; EA.hy926: n=28/8, HeLa: n=39/8, and HUVEC: n=14/8), piceatannol (green columns; EA.hy926: n=17/6, HeLa: n=59/13, and HUVEC: n=18/9), or oligomycin A (blue columns; EA.hy926: n=24/5, HeLa: n=25/7, and HUVEC: n=13/9).



**Fig. 3.** Concentration response curve of resveratrol-mediated enhancement of histamine- (100  $\mu$ M) evoked mitochondrial  $Ca^{2+}$  uptake in EA.hy926 cells (n=17-22/3).

**Fig. 4.**

Representative SIM images of EA.hy926 (left panel) and HUVEC (right panel) cells expressing DIER (green) and stained with MitoTrackerRed® CMXRos (red), lower panels represent white boxes from upper panels (A). Co-localization levels of endoplasmic reticulum and mitochondria in EA.hy926 (n=27/12) and HUVEC (n=27/10) cells presented as Manders 2 (left panel) as well as Pearson (right panel) coefficient (B). Representative 3D reconstructions (upper panel: top view; lower panel: side view) of confocal fluorescence-stacks of HeLa cells expressing DIER (green) and mtDsRed (red) under control conditions or with combined overexpression of AKAP-RFP-CAAX (C). Overlapping area of endoplasmic reticulum and mitochondria in HeLa with (n=65/6) or without (n=66/6) overexpression of AKAP-RFP-CAAX construct shown as Manders 2 (left panel) as well as

Pearson (right panel) coefficient (D). Representative curves (left panels) show mtCa<sup>2+</sup> uptake, measured by 4mtD3cpv, in response to 100 μM of histamine (His) in Ca<sup>2+</sup>-free solution in Ea.hy926 (E) and HeLa (F) cells overexpressing AKAP-RFP-CAAX without compound treatment (black curves) as well as after incubation with 100 μM resveratrol (red curves), 100 μM piceatannol (green curves) or 10 μM oligomycin A (blue curves). Bars (right panels) represent an average of maximal ratio signals (mean ± SEM) of IP<sub>3</sub> generating agonist response of Ea.hy926 and HeLa cells overexpressing AKAP-RFP-CAAX under control conditions (white columns; EA.hy926: n=20/9 and HeLa: n=18/6) as well as after treatment with resveratrol (red columns; EA.hy926: n=17/6 and HeLa: n=23/6), piceatannol (green columns; EA.hy926: n=14/5 and HeLa: n=21/6), or oligomycin A (blue columns; EA.hy926: n=18/5 and HeLa: n=20/5).

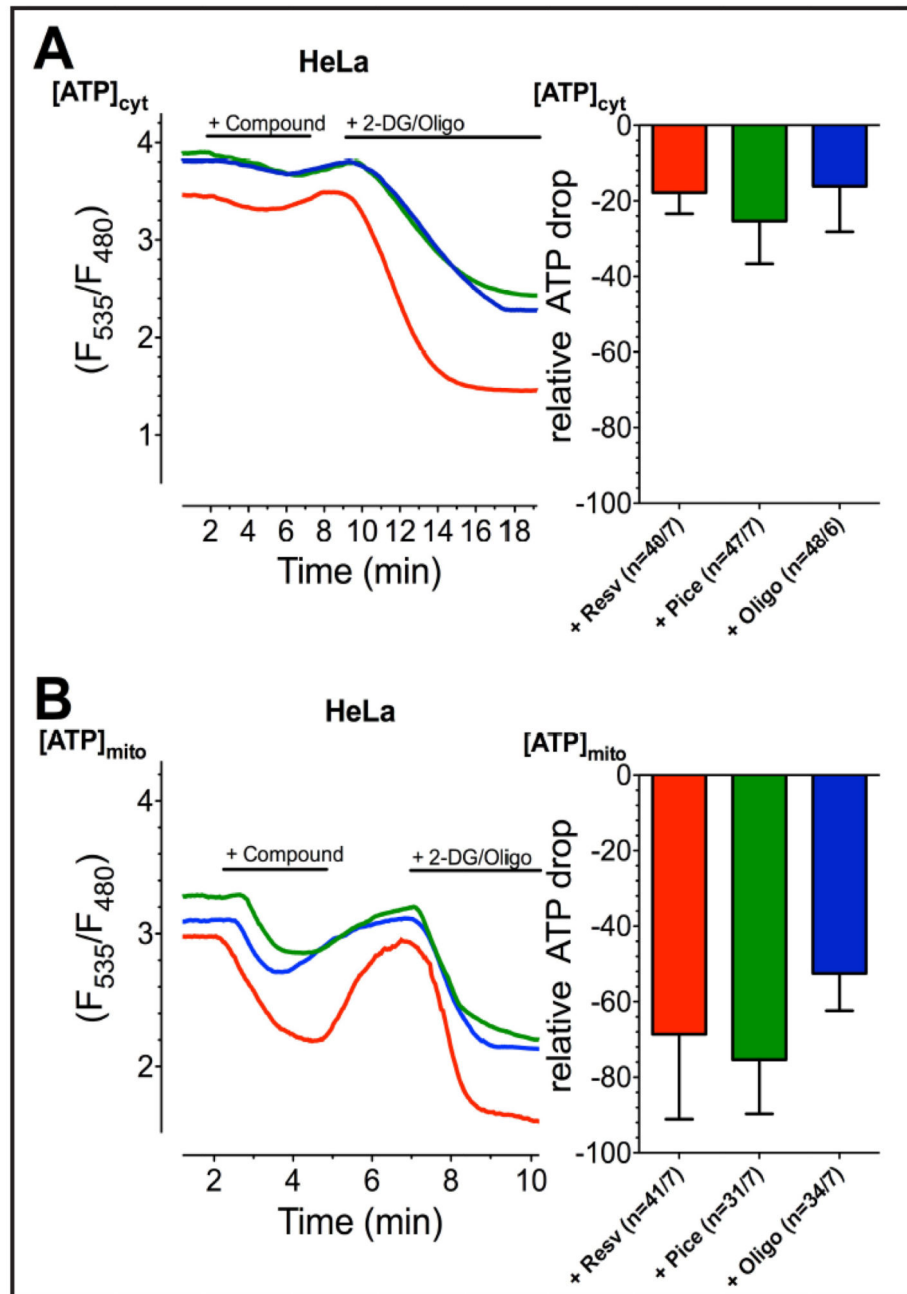


**Fig. 5.** Representative curves (left panels) show cytATP (A) and mtATP (B) ratio signals of HeLa cells, measured by AT1.03 targeted to cytosol or mitochondria, respectively, stimulated with first 100  $\mu\text{M}$  resveratrol (red curves), 100  $\mu\text{M}$  piceatannol (green curves), or 10  $\mu\text{M}$  oligomycin A (blue curves) and afterwards with 2.5 mM 2-DG and 10  $\mu\text{M}$  oligomycin A in order to gain a complete depletion of ATP. Bars (right panels) reveal average ratio signals to resveratrol (red columns; cytATP: n=40/7, mtATP: n=41/7), piceatannol (green columns; cytATP: n=47/7, mtATP: n=31/7) or oligomycin A (blue columns; cytATP: n=48/6, mtATP:

n=34/7), presented as percentage of complete ATP depletion. The cells' response to the combination of 2.5 mM 2-DG and 10  $\mu$ M oligomycin A was set to 100 %.

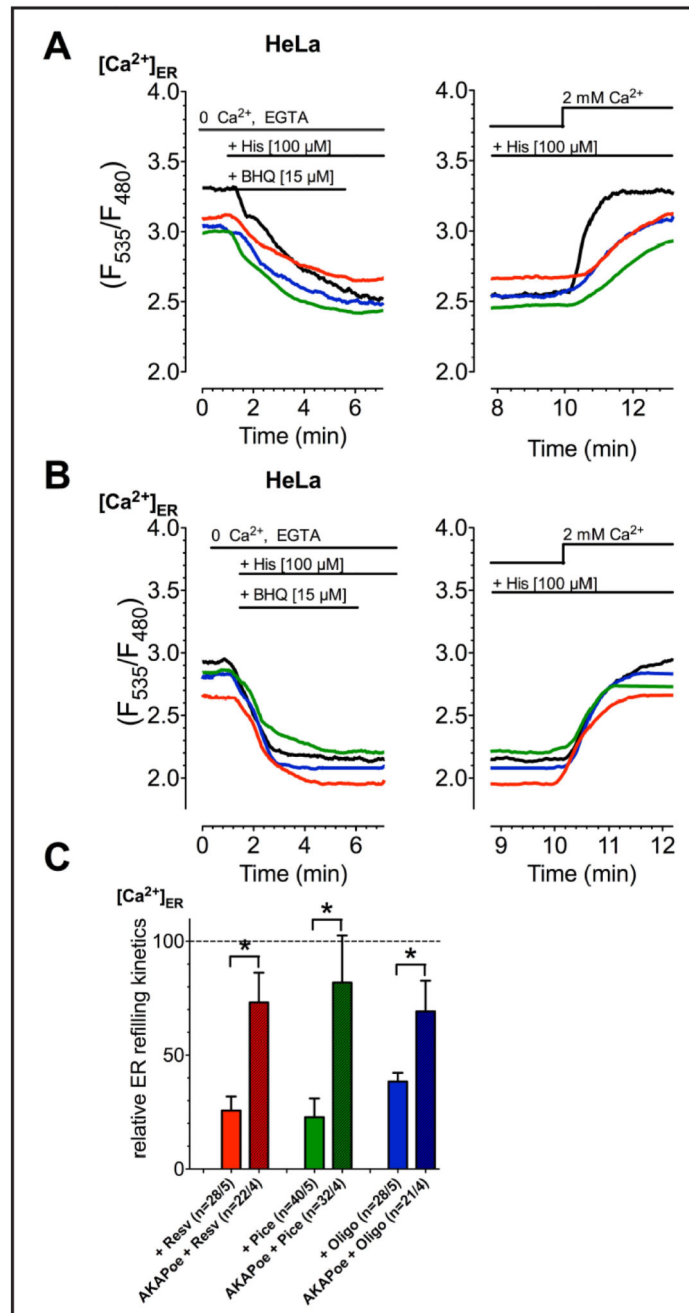


**Fig. 6.** Representative curves reflect ER  $Ca^{2+}$  ratio signals over time of HeLa cells without (A) or with (B) overexpression of AKAP-RFP-CAAX (AKAPoe), measured by D1ER. The ER  $Ca^{2+}$  store was depleted using 100  $\mu M$  histamine (His) and 15  $\mu M$  BHQ in  $Ca^{2+}$ -free EGTA-buffered solution. Then the cells were incubated with compounds (resv: red curves, pice: green curves; oligo: blue curves) or kept in compound-free solution (black curves) and afterwards external  $Ca^{2+}$  [2 mM] was added. The slope of the cells' ER  $Ca^{2+}$  uptake after 100  $\mu M$  resveratrol (red columns; Resv: n=28/5, AKAPoe+Resv: n=22/4), 100  $\mu M$

piceatannol (green columns; Pice: n=40/5, AKAPoe+Pice: n=32/4) or 10  $\mu$ M oligomycin A (blue columns; Oligo: n=28/5, AKAPoe+Pice: n=21/4) incubation was normalized to corresponding control conditions and presented as percentage of ERCa<sup>2+</sup> uptake slope of control (C).

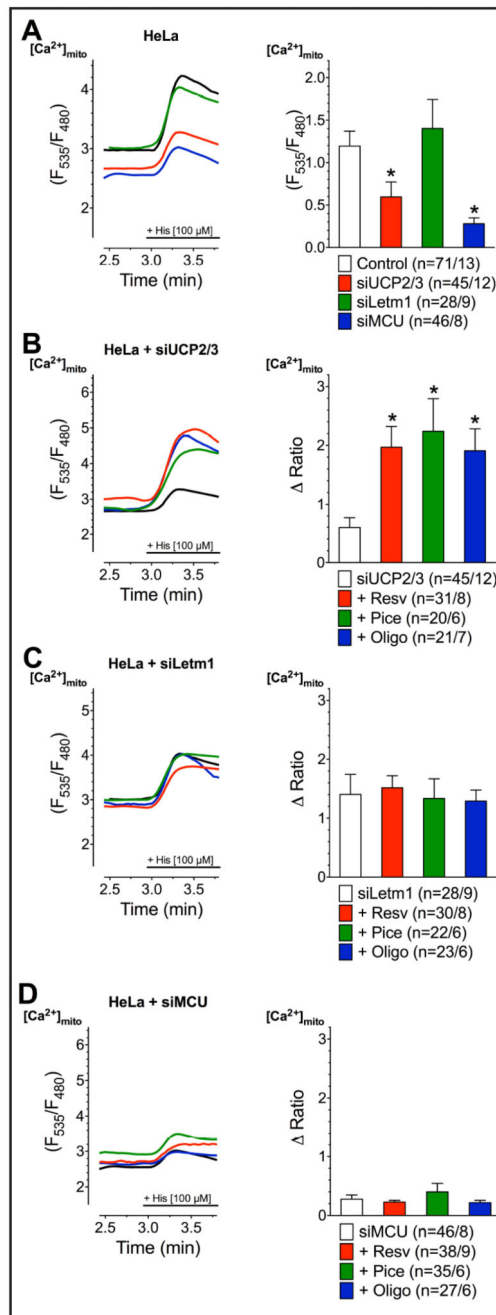


**Fig. 7.** Representative curves (*left panels*) reflect  $mtCa^{2+}$  ratio signals upon 100  $\mu$ M histamine (His) addition in  $Ca^{2+}$ -free solution of HeLa cells with transient knockdown of UCP2/3 (A), Letm1 (B) or MCU (C) after treatment with 100  $\mu$ M resveratrol (red curves), 100  $\mu$ M piceatannol (green curves) or 10  $\mu$ M oligomycin A (blue curves) as well as under control conditions with corresponding knockdown (black curves) or without knockdown (dotted lines). Bars (*right panels*) represent an average of maximal  $[Ca^{2+}]_{mito}$  ratio signals of  $IP_3$  agonist stimulated response of cells without knockdown (dotted columns; n=71/13), under

corresponding control conditions (white columns; siUCP2/3: n=47/12, siMCU: n=46/8, siLetm1: n=28/9) or after treatment with resveratrol (red columns; siUCP2/3: n=31/8, siMCU: n=38/9, siLetm1: n=30/8), piceatannol (green columns; siUCP2/3: n=20/6, siMCU: n=35/6, siLetm1: n=22/6) or oligomycin A (blue columns; siUCP2/3: n=21/7, siMCU: n=27/6, siLetm1: n=23/6).

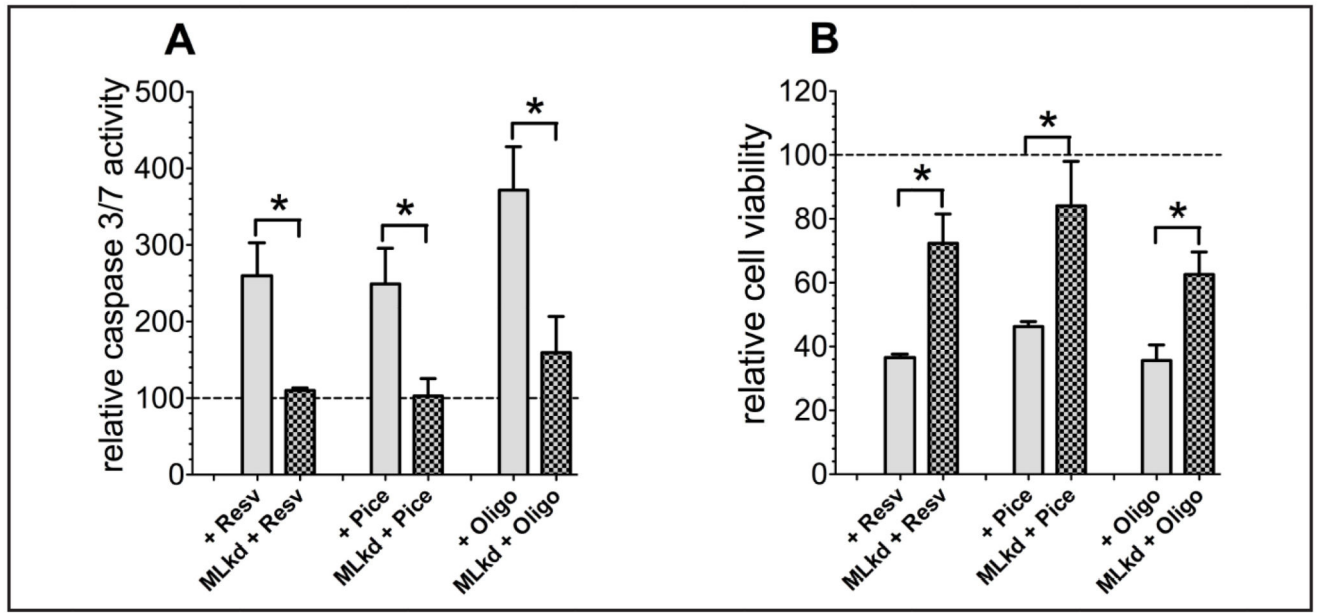


**Fig. 8.**

Caspase activity of control HeLa cells or HeLa cells with combined knockdown of MCU and Letm1, normalized to corresponding control conditions as percentage of viable cells, was measured via Caspase 3/7-Glo assay following the standard protocol after 36 h of compound incubation (A). Cell viability of control HeLa cells or HeLa cells with combined knockdown of MCU and Letm1 was determined using Celltiter-Blue assay according to the standard protocol after 36 h of incubation with resveratrol [100  $\mu$ M], piceatannol [100  $\mu$ M], or oligomycin A [10  $\mu$ M] and calculated as percentage of viable cells in comparison to corresponding control cells (B).

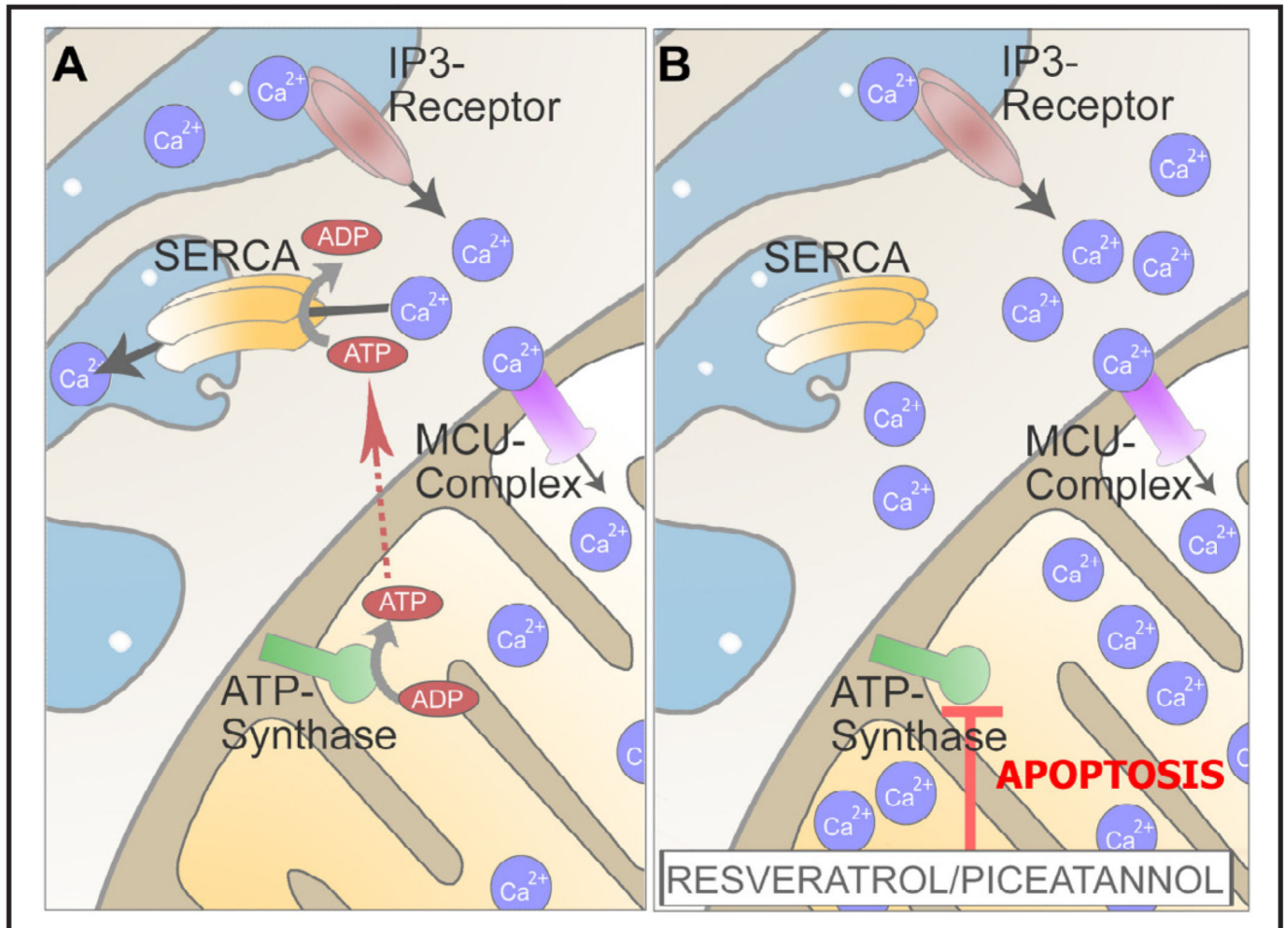


**Fig. 9.** Schematic illustration of the described effect of resveratrol and piceatannol on mitochondrial  $Ca^{2+}$  handling and consequences thereof. Cancer cells have an enforced ER-mitochondria tethering to meet the cancer cells energy demand and to fuel SERCA for efficient uptake of intracellularly released  $Ca^{2+}$  (A). By their inhibitory effect on ATPsynthase, resveratrol and piceatannol yield decreased SERCA activity that, in turn, results in an enhanced mitochondrial  $Ca^{2+}$  uptake,  $Ca^{2+}$  overload, and, ultimately apoptotic, cell death in cancer cells (B).